





JOURNAL OF ENGINEERING SCIENCES

2-D Geometric Accuracy Investigation of Vat-Photopolymerisation Printed Yttrium Stabilised Zirconia Ceramics

Fatih Tarak*a, Basar Ozkan b, Ehsan Sabetc

Submitted: 03.12.2024 Revised: 28.04.2025 Accepted: 16.05.2025 doi:10.30855/gmbd.070525A02

ABSTRACT

Keywords:

Ceramic additive manufacturing, vatphotopolymerisation, yttrium stabilised zirconia, dimensional accuracy Vat-photopolymerisation is among the most promising approaches in ceramic additive manufacturing due to its low production costs and high dimensional accuracy. However, because the printing method is based on a photopolymerisation reaction initiated by a light source, light scattering significantly affects the quality of printed parts. This issue is particularly pronounced in ceramics with high refractive indices, such as yttrium stabilised zirconia (Y2O3-ZrO2), where achieving precise geometric accuracy becomes challenging due to increased light scattering. To address this, the cure depth and two-dimensional accuracy of ceramic suspensions were evaluated. The study examined two different particle sizes to assess their influence on dimensional accuracy due to varying levels of light scattering. Additionally, since the photopolymerisation process in ceramic suspensions is initiated by free radicals, various concentrations of photoinitiators were tested to determine their impact on both cure depth and geometric error. Both particle size and photoinitiator concentration were analysed under different exposure times to assess their effects on the printed parts. Low photoinitiator concentration ceramic suspensions achieve the lowest error of 0.182 mm and 0.375 mm with small and large ceramic particles respectively. The results demonstrate that particle size and photoinitiator concentration play critical roles in determining the cure depth and geometric accuracy of ceramic green bodies.

1. Introduction

One of the primary advantages of additive manufacturing (AM) for ceramic production is its ability to achieve high precision in fabricating complex geometries, a capability often beyond the reach of traditional manufacturing methods [1]. Various printing methods such as powder based selective laser sintering (SLS) or fused deposition modelling (FDM) were established in the literature to build ceramic parts [2]. Vat-photopolymerisation occupies a unique position among the various AM ceramic techniques for ceramics due to its benefits, such as lower printing costs and precise manufacturing enabled by high-definition light sources [3]. Owing to its high surface quality and printing precision, ceramic vat photopolymerisation is widely preferred in advanced industries such as defence, aerospace, electronics and biomedical [4–6]. Vat photopolymerisation methods can be categorised into two types based on the movement direction of the build platform: top-down and bottom-up approaches. In the top-down technique, the light source is positioned above the vat, and the build platform moves downward into the resin vat after each layer is printed [7]. A scraper is employed to evenly

a' Wolfson School of Mechanical, Electrical & Manufacturing Engineering, Loughborough University, Loughborough, LE11 3TU, United Kingdom, Orcid: 0000-0002-0343-9313

Department of Materials, Loughborough University, Loughborough LE11 3TU, United Kingdom, Orcid: 0000-0003-0283-6322

Additive Manufacturing Centre of Excellence, 33, Shaftesbury Street South, Derby, DE23 8YH, United Kingdom, Orcid; 0000-0001-8083-6155 Corresponding author: f.tarak@lboro.ac.uk

distribute fresh resin over the previously cured layer, ensuring a consistent layer thickness. Conversely, in the bottom-up approach, the light source is located beneath a transparent vat bottom, and the build platform moves upward by a distance equal to the predefined layer thickness after each layer is formed. A scraper is generally not required in this method, unless the resin exhibits high viscosity [8].

Both printing approaches possess distinct advantages and disadvantages. The top-down method necessitates a significantly larger volume of resin to fill the entire vat, which can be material-intensive and costly [9]. In contrast, the bottom-up technique is more material-efficient; however, it introduces challenges associated with the peeling force that arises during the separation of the cured layer from the bottom of the vat. These forces can potentially lead to print defects or mechanical stress on the printed part which may cause failure during the printing process or subsequent postprocessing stages [10]. The type of light source utilised in additive manufacturing varies depending on the printer and the specific application. In the top-down approach, laser and digital light processing (DLP) light sources are predominantly employed. Conversely, in the bottom-up method, liquid crystal display (LCD) screens are often used, either independently or in conjunction with DLP projectors. Laser light sources, due to their fine beam dimensions, offer superior dimensional accuracy in the lateral direction. However, the narrow beam must scan the entire area to cure the photo-sensitive resin, resulting in a more complex printing process with additional parameters. This scanning approach is also time-consuming, particularly for larger components. In contrast, LCD and DLP light sources expose the entire layer simultaneously, which not only significantly increases the printing speed but also promotes the formation of more uniform polymer chains [11]. Although high-resolution LCD screens are available, DLP projectors generally offer superior resolution due to their structural design. In DLP systems, the ultraviolet (UV) light source is directed using a digital micromirror device (DMD), which consists of micromirrors measuring approximately 16 µm, fabricated from aluminium and controlled via a complementary metal-oxide-semiconductor (CMOS) circuit [12]. The micromirrors operate in an "on-off" mode, reflecting the UV light to project high-resolution images onto the DLP screen. In the light spectrum, UV light encompasses wavelengths between 100 nm and 400 nm. However, in vat photopolymerisation processes, most UV light sources operate at a wavelength of 405 nm, which lies at the boundary between ultraviolet and visible light, in order to initiate the polymerisation of photo-sensitive resins.

The printing method relies on a photopolymerisation reaction, which is a chain reaction initiated by a light source [13]. A photocurable binder mixture—comprising monomers, oligomers, and other additives such as photoinitiators—is mixed with ceramic powder to form a photosensitive ceramic suspension [14]. Upon exposure to light, the ceramic slurry cures, entrapping the ceramic particles within the polymer network. As a result, polymer-ceramic composite parts are produced as a green body [15]. The polymer structure is subsequently removed through post-processing to obtain dense ceramic bodies. However, even though most of the ceramic suspensions have high solid loading ranging from 35 vol.% to 50 vol.% depending on powder characteristic, binder mixture has significant importance on the product [16].

The selection of binder resin components is primarily based on the viscosity, molecular weight, and functionality of the monomers and oligomers that consist of repeating monomer units. The viscosity of the monomers and oligomers directly affects the overall viscosity of the resin, and consequently, the ceramic suspension [17]. Although viscosity is not critically important in top-down printing methods, it is a significant parameter in bottom-up approaches, which are more sensitive to changes in suspension viscosity. Extremely low slurry viscosity can lead to instability of ceramic particles within the suspension, whereas high viscosity increases the peeling force during the printing process [18]. Excessive peeling forces can lead to print failure and increase interlayer stresses, potentially resulting in delamination or cracking after printing. Consequently, maintaining the suspension viscosity below 5000 mPa·s is recommended in the literature [19].

Another important consideration in selecting resin monomers and oligomers is their functionality. Functionality refers to acrylate functionality, which denotes the total number of alkene (C=C double) bonds present in a molecule [14]. During the photopolymerisation process, these alkene bonds break and form covalent bonds with other reactive carbon atoms, resulting in C-C single bonds and the formation of longer polymer chain networks. Highly functional molecules are capable of creating more complex, cross-linked polymer networks, whereas difunctional monomers or oligomers (with two functional groups) typically form linear chain networks. Monofunctional molecules (with a single functional group),

by contrast, are only able to form simple polymer networks. Therefore, the number of alkene bonds in the molecule directly correlates with the potential complexity of the polymer network and thus influences the mechanical properties of the resulting green body [20]. However, highly functional monomers and oligomers tend to have larger molecular structures, which generally leads to increased viscosity compared to molecules with fewer functional groups. Moreover, the use of excessively high-functional compounds can result in greater volumetric shrinkage due to the higher molecular density as monomers are converted into polymer networks. This, in turn, may produce more brittle green bodies [14].

To address these challenges, many studies have employed combinations of monomers and oligomers with varying functionalities to optimise both the viscosity, and the mechanical properties of the binder resin used in ceramic suspensions. Numerous studies have been undertaken to select and optimise binder components for various ceramic powders, given their direct influence on the properties of the manufactured parts [20]. A comprehensive study developed 52 distinct formulations and tested to produce high-precision silica (SiO₂) cores for investment casting applications [21]. A subsequent study by the same authors investigated the types and characteristics of monomers/oligomers, along with their concentrations, in relation to key parameters such as suspension viscosity, tensile strength, and post-processing performance. High geometric accuracy in all directions with a complex core geometry and adequate mechanical properties for advance industries like aerospace achieved with the final study [15]. Similarly, in a different comprehensive investigation, six monomers/oligomers were initially tested in their pure forms to assess the properties of the resulting green bodies. A mixture comprising three monomers demonstrated favourable material properties, including appropriate viscosity, tensile strength, and minimal shrinkage. This optimised formulation was subsequently combined with alumina (Al₂O₃) powder and subjected to printing processes [22]. Similar to the bottom-up approach, the optimisation of binder resin components is also essential in top-down printing processes. In this study, three different resin components with varying functionalities were investigated by formulating eleven distinct resin compositions for zirconia (ZrO₂) ceramic powder. A combination of mono-, bi-, and tri-functional monomers was employed in a ratio of 3.5:3.5:3, along with the addition of 1 wt.% of a monofunctional long-chain surface modifier. A high solid loading of 52 vol.% zirconia powder was incorporated into the optimised binder resin and processed using a laser-based top-down printer. The resulting printed parts exhibited enhanced mechanical properties, demonstrating the effectiveness of the formulation strategy [23]. Due to its critical influence on parts regarding to the literature, binder formulation development for yttria-stabilised zirconia ceramics was carried out by examining four different monomers/oligomers at varying concentrations, following a full factorial design of experiments in the previous work. Generated 27 formulations were investigated regarding their viscosity and mechanical properties as binder only and selected formulation was subject of a loading study. The viscosity of ceramic loading of 40 vol.%, 45 vol.% and 50 vol.% were measured and optimum loading amount defined [24].

On the other hand, achieving high geometric accuracy when printing ceramics with high refractive indices (RI), such as zirconia, remains challenging due to their optical behaviour, specifically light scattering [25]. Light scattering is directly correlated with the refractive index differences between the liquid resin and the ceramic powder. To this end, the development of high-refractive-index binders has been investigated for Si₃N₄ ceramics in order to control and enhance curing depth as well as horizontal resolution [26]. The redirection of light by ceramic particles occurs through three main mechanisms: diffraction, reflection, and refraction. Reflection and refraction occur when light interacts directly with the particle; in reflection, light is redirected back after striking the particle's surface, while in refraction, the light changes direction as it travels through the particle. In contrast, diffraction does not involve direct contact between light and the particle; instead, the light alters its path as it passes near the particle within the scattering volume [27]. Since ceramic suspensions are typically highly loaded with ceramic powders, light scattering becomes particularly significant for materials with high refractive indices, such as zirconia [28]. In addition to the optical properties of ceramic suspensions, the chemical composition of the suspension, which influences the polymerisation chain reaction, is crucial for achieving high-precision ceramic printing [11].

Selection and concentration of the photoinitiator (PI), which is responsible for generating free radicals to initiate crosslinking, as well as the presence of other additives, must be carefully optimized [17]. Various types of photoinitiators and their combinations have been investigated, particularly in the context of vat-photopolymerisation applications like

dental industry. Among these, 2,4,6-trimethylbenzoyl phosphine oxide (BAPO) demonstrates adequate mechanical properties within a short curing time, which is directly associated with the degree of monomer-to-polymer conversion. Consequently, BAPO proves its effectiveness in enhancing the green body's quality and curing efficiency [18]. BAPO and 2,4,6-trimethylbenzoyl-diphenyl phosphine oxide (TPO) are the most commonly used UV photoinitiators for acrylate-based resins [17]. A Taguchi design of experiments (DoE) approach was employed to investigate the effects of the photoinitiator (BAPO) and other formulation components on the printability of a biocompatible resin material [29]. The effect of TPO concentration, ranging from 1 wt.% to 4 wt.%, was studied in conjunction with varying exposure times (1 to 8 seconds) in cordierite (2MgO·2Al₂O₃·5SiO₂) ceramic suspensions. The curing depth of the ceramic slurry, under a fixed light intensity of 7.79 mW/cm², increased with higher photoinitiator concentrations and reached a maximum at 2 wt.%. Beyond this concentration, the curing depth decreased across all exposure times [19].

Furthermore, printing parameters such as light intensity and exposure time require precise calibration to produce accurate ceramic green bodies [30]. The effects of printing parameters such as exposure time, print orientation, and layer thickness are well-established in the literature for vat photopolymerisation of resin-based systems [31,32]. A mathematical framework was developed to simulate the cure kinetics of vat photopolymerisation in the fabrication of microelectronic components. Dimensional polymerisation shrinkage was examined in relation to the dimensional accuracy of the green body, in order to understand the influence of printing parameters and to optimise and predict them accordingly [33]. A Taguchi design of experiments was conducted to investigate the printing parameters of vat-photopolymerisation resin printing. Layer thickness, orientation, and exposure time were examined through nine different experiments. Dimensional changes of various shapes on the test body were measured, and the printing parameters were subsequently optimised [32].

Similarly, a more comprehensive Taguchi experimental design was implemented, incorporating twelve different printing parameters. In addition to the parameters considered in previous work, separation speed, approach speed, and overlift distances were included in the study. The effects of layer thickness, orientation, and exposure time were again found to significantly influence the dimensional accuracy of the green parts, consistent with earlier findings [31]. However, the number of studies focusing on print parameter optimisation with ceramic suspensions in vat-photopolymerisation remains limited. Four different light intensities, ranging from 24 mW/cm 2 to 96 mW/cm 2 , were evaluated alongside varying exposure times to investigate the dimensional accuracy of alumina suspensions through the printing of 5 mm × 5 mm square specimens. The optimal printing parameters were identified as a light intensity of 60 mW/cm 2 combined with an exposure time of 5 seconds.

These conditions were subsequently applied to print the test geometry, yielding a maximum geometric deviation of 0.04 mm, as determined via X-ray computed tomography (XCT) analysis [34]. A brief study was conducted using a zirconia ceramic suspension to investigate the effect of post-printing on dimensional shrinkage. Approximately 25% shrinkage was observed with a 73 wt.% loaded ceramic suspension printed at a 20 μ m layer thickness [35]. Similarly, an 84 wt.% loaded zirconia ceramic slurry was printed using a laser-based vat photopolymerisation process and evaluated for its mechanical properties, dimensional accuracy, and surface roughness in the context of dental applications. Among the two printed orientations, horizontally printed parts exhibited the lowest dimensional error in the vertical direction, as expected. In addition to shrinkage considerations, the horizontally printed group also achieved the best surface quality, with a surface roughness value of 0.7 R_a [36]. A DLP-based printer was used to fabricate a 44 vol.% ceramic-loaded zirconia suspension. Although adequate rheological characteristics and mechanical properties were achieved, gaps smaller than 200 μ m and holes smaller than 300 μ m could not be printed using the selected exposure energy of 150 mJ/cm², due to significant overcuring effects [37]. Due to their critical impact on both dimensional precision and the photopolymerisation reaction, printing parameters—such as exposure energy (the product of light intensity and exposure time), layer thickness, and print orientation—should be systematically investigated for each specific ceramic material [11].

The characteristics and morphology of ceramic particles have a direct influence on the properties of the green body, as well as the overall quality of the final product, including geometric accuracy and surface finish. Despite its significance,

this topic has not been studied as extensively as other parameters related to dimensional precision and surface quality. Although not directly attributed to powder morphology, high surface quality and a geometric error of only 0.05 mm were achieved in the printing of micro-ceramic gears using a mixture of micron-sized zirconia and nano-sized alumina powders.

However, these results were obtained with a low solid-loading suspension, which reduces light scattering but results in increased shrinkage during post-processing [38]. The type of ceramic powder plays a critical role due to its direct interaction with light. For darker ceramics such as SiC or Si_3N_4 , a reduction in particle size tends to improve lateral dimensional accuracy. In contrast, for more opaque ceramics with lower refractive indices, such as hydroxyapatite, finer particles reduce curing depth and increase horizontal dimensional error [39]. In another study, the particle size distribution of alumina ceramic was refined through the addition of nano-sized zirconia powder. As the proportion of nano-zirconia increased from 0% to 20%, the curing depth of the ceramic suspension decreased from 150 μ m to 100 μ m [28]. The most comprehensive investigation into the interaction between ceramic powders and light in stereolithography was conducted using alumina ceramics. Mie scattering theory was applied and simulated using the finite element method (FEM) to explore particle-light interactions during exposure.

The study examined various particle size distributions, input energy levels, and refractive index differences. Simulation results demonstrated that an increase in particle size led to a broader curing width, even when the simulation was performed with a narrow light beam [40]. A similar study modelled vat photopolymerisation using a mathematical framework. It considered various polygonal alumina particle shapes in both two-dimensional and three-dimensional spaces, incorporating specific degrees of rotational orientation [41].

This study investigates the two-dimensional accuracy of yttria-stabilised zirconia ceramic green bodies, with a particular focus on dimensional deviations in the horizontal direction, as a continuation of previous research on binder development [24]. Given the limited information available in the literature, the influence of yttria-stabilised zirconia particle size on light scattering is evaluated, with the aim of understanding its effect on lateral dimensional accuracy and curing depth. Furthermore, the concentration of the photoinitiator within the ceramic slurry is examined, owing to its critical role in the photopolymerisation reaction, across a range of concentrations. Finally, the impact of varying exposure times under fixed light intensity is assessed to determine the effect of light energy on curing behaviour in all directions, with a focus on both curing depth and dimensional precision.

2. Materials and Methods

The binder resin and dispersant for the ceramic suspension were selected based on previous studies on binders [24] and dispersants [18], as outlined in Table 1, along with their respective concentrations in the mixture. Difunctional 1,6-hexanediol diacrylate (HDDA) and multifunctional dipentaerythritol hexaacrylate (DPHA) were purchased from Miwon Bldg. (Gyeonggi-do, Korea), while the monofunctional monomer N-vinyl-2-pyrrolidone (NVP) was supplied by BASF (Ludwigshafen, Germany). Additionally, a urethane methacrylate with two functional groups, Genomer 4247, sourced from Rahn AG (Zürich, Switzerland), was incorporated into the photosensitive resin. BYK-111 was added to the ceramic suspension at 3 wt.% relative to the content of yttrium-stabilised zirconia powder, in accordance with literature recommendations [23]. Phenylbis (2,4,6-trimethylbenzoyl) phosphine oxide (BAPO) (Rahn AG, Zürich, Switzerland) was utilized as the photoinitiator (PI) to initiate the polymerisation chain reaction under UV light irradiation.

Table 1. Formulation of photocurable resin mixture

Name Concentration (wt.%)		
NVP	5	
HDDA	58	
DPHA	5	
Genomer 4247	32	

The desired photocurable formulations were prepared by mixing yttrium-stabilised zirconia powder (Isik Tech, Izmir, Türkiye) at a 40 vol.% solid loading, based on the designed photoinitiator concentration and particle size. The particle size distribution of powders is measured (LA-950 laser scattering particle size distribution analyser, Horiba Ltd., Kyoto, Japan) and represented in Table 2. A planetary mixer (SpeedMixer DAC 150 FVZ, Hauschild, Germany) was used for 30 min at 2000 rpm to sustain homogenous and agglomeration free ceramic suspensions.

Table 2. Yttrium stabilised zirconia powder particle size

Powder Name	d ₃₀ (μm)	d ₅₀ (μm)	d ₉₀ (μm)
Isik YSZs	0.1410	0.1830	0.3012
Isik YSZl	0.5815	0.7290	1.3774

3 mol % yttrium stabilised zirconia $(Y_2O_3-ZrO_2)$ with two different particle sizes were investigated with various photoinitiator concentrations to understand the effect of the particle size and photoinitiator concentration on dimensional accuracy and cure depth in ceramic vat-photopolymerisation. Various exposure times (20s, 50s, 100s) were tested with a bottom-up printer (5.5 mW/cm²) to investigate the print parameter on 2-D geometric error. All factors and levels are demonstrated in Table 3.

Table 3. Factors and levels of designed experiments

Factor	Level 1	Level 2	Level 3
Particle Size (nm)	183	729	-
Photoinitiator (wt.%)	0.1	0.15	0.25
Exposure Time (s)	20	50	100

2-D dimensional accuracy of the ceramic suspension formulations was tested with a ring shape with 15mm and 20mm internal and external diameters (Figure 1). Dimensional error calculations were conducted with equation **Hata! Başvuru kaynağı bulunamadı.** where r_i and r_e are internal and external measured radiuses by a stereo microscope (Omni, ASH Vision, Ireland).

$$Dimensional Error = |(r_e - r_i) - 2.5|$$
 (1)

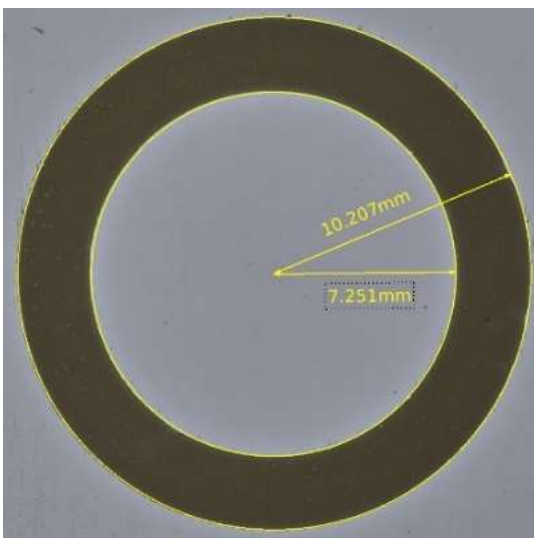


Figure 1. 2-D dimensional error ring test

3. Results and Discussion

The dimensional accuracy of ceramic green bodies produced by vat-photopolymerisation primarily depends on the efficiency of the polymerisation reaction initiated by a light source. However, unintended light irradiation can trigger

irreversible polymerisation in undesired regions of the ceramic slurry, a phenomenon known as overcuring. It typically arises due to light scattering within the mixture or backlight effects caused by excessively long UV exposure. The primary cause of light scattering is the difference in refractive indexes (RI) between the photosensitive resin and the yttrium stabilised zirconia ceramic powder [42]. Significant disparities in refractive indices also influence the cure depth (Cd) of the mixture, as described by the Beer-Lambert law equation (Equation 2) where (Δn) represents the differences of refractive indexes [43].

$$C_d = \frac{2}{3} x \frac{d}{\varphi \beta \Delta n^2} x \ln \left(\frac{E_0}{E_c} \right)$$
 (2)

Dimensional error results calculated by equation Hata! Başvuru kaynağı bulunamadı. are monitored in Table 4. As anticipated, larger particles resulted in greater geometric error due to increased light scattering. Big particles scatter more light photons because of their size, whereas the likelihood of scattering by smaller particles is lower. It is important to note that light redirection is not solely dependent on photon-particle interaction; the scattering volume of particles is also larger than their actual physical volume [27]. Since all mixtures were loaded with the same volumetric particle content, the scattering volumes of smaller particles overlap within a given space, reducing overall scattering through diffraction [27]. The influence of particle size becomes more evident in mixtures containing 0.1 and 0.15 wt.% photoinitiator under short exposure times, where smaller particles exhibit reduced scattering, even though their surface area per unit volume is increased [28]. However, higher photoinitiator concentrations and longer exposure times tend to reduce the influence of particle size on light scattering. Although the parameter d in the Beer-Lambert law represents particle diameter, significant changes in cure depth between different particle sizes were not observed. The effects of light scattering and photoinitiator (PI) content may have outweighed the influence of particle size on cure depth, with the variation in cure thickness being approximately 10-20 μ m. Measurement errors must be taken into account when considering these relatively minor differences.

Table 4. Dimensional error of ceramic suspensions with selected particle size and photoinitiator amount under various exposure times

Powder Name	Photoinitiator (wt.%)	Exposure Time (s)	Dimensional Error (mm)
	0.1	20	0.182
		50	0.656
		100	0.956
	0.15	20	0.55
Isik YSZs		50	0.971
		100	1.396
	0.25	20	0.831
		50	1.37
		100	1.849
Isik YSZl	0.1	20	0.375
		50	0.727
		100	1.05
	0.15	20	0.677
		50	1.079
		100	1.536
	0.25	20	0.622
		50	1.119
		100	1.578

Despite the fact that higher concentration of photoinitiator enhances the absorption of UV light by photoinitiator particles, increased photoinitiator concentration in the ceramic slurry also raises the density of free radicals during UV exposure. As a result, curing may extend beyond the intended printing volume, leading to significant overcuring in the ceramic green body. This trend is clearly visible in the results for fine particles shown in Figure 2. Specifically, 40-45% constant increase in dimensional error demonstrates an almost linear relationship between photoinitiator content and dimensional error of fine particles (Table 4). However, while the dimensional error increases by approximately 50% when the photoinitiator content rises from 0.1 wt.% to 0.15 wt.%, it stabilizes with further photoinitiator additions when using

coarse powder particles, as shown in Figure 3. This indicates that the mixtures with coarse particles exhibit the highest dimensional error, which does not increase further even with additional photoinitiator in the slurry.

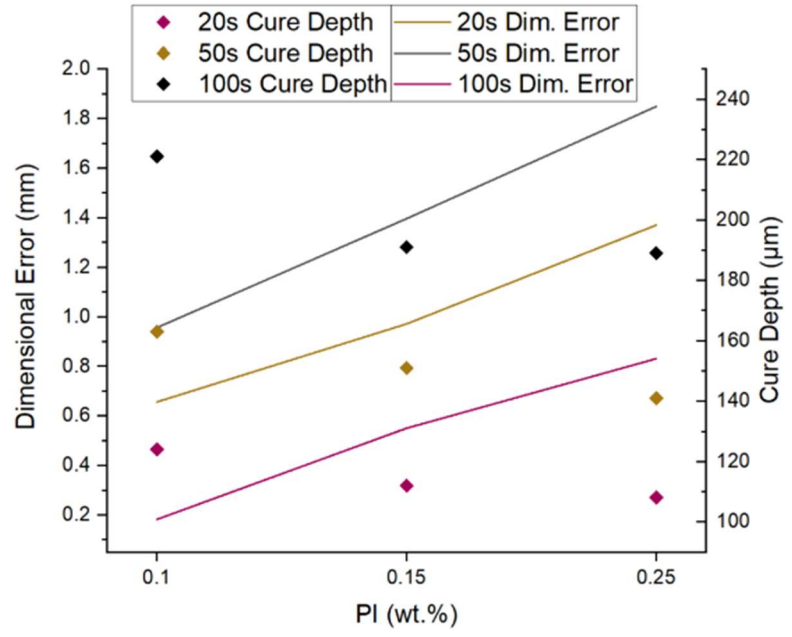


Figure 2. Dimensional Error and Cure depth results of Isik YSZs Zirconia powder with various exposure times and photoinitiator concentrations

Conversely, cure depth decreased with the increasing photoinitiator concentration in the slurry across all particle sizes. This reduction in cure depth may be attributed to the higher absorption of UV light during free radical generation, or possibly due to rapid curing at the surface, which blocks UV photons from penetrating deeper into the material [44]. The results suggest that low photoinitiator concentrations can achieve sufficient cure depth while minimising dimensional errors for both small and large particle sizes.

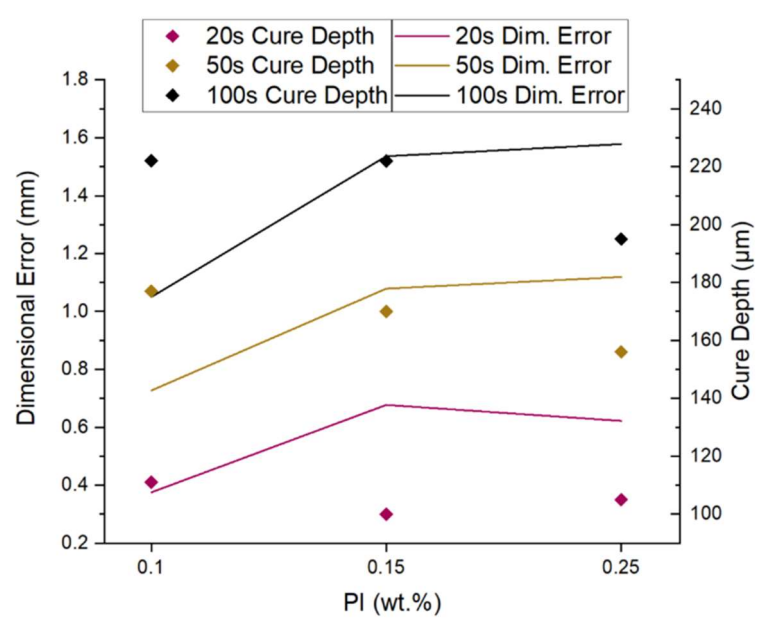


Figure 3. Dimensional Error and Cure depth results of Isik YSZl Zirconia powder with various exposure times and photoinitiator concentrations

Exposure time was examined to assess the effect of light energy on the polymerisation mechanism. The light energy was calculated as the product of light intensity (mW/cm^2) and exposure time (s), resulting in the total energy delivered per unit area (mJ/cm^2) . For this study, light intensity was held constant at 5.5 mW/cm^2 , while light energy was varied by adjusting exposure times. As expected, lower geometric error was observed with shorter exposure times due to the reduced

light energy exposure. As shown in both Figure 2 and Figure 3 the dimensional error curves shift upward with increased exposure time, following a similar trend. This confirms that higher light energy accelerates the crosslinking process, leading to greater error regardless of particle size. Additionally, cure depth for both particle sizes displayed similar behaviour with varying exposure times, further supporting the Beer-Lambert law, as described in equation 2 where E_0 and E_0 and E_0 are represent the initial and critical energy of the light source, respectively [43].

In view of the potential applications of yttrium-stabilised zirconia in the biomedical and dental fields, an optimised formulation was printed. Figure 4 depicts the printed open source dental crown [45] and dental implant [46], both of which demand exceptional geometric precision and enhanced mechanical performance.

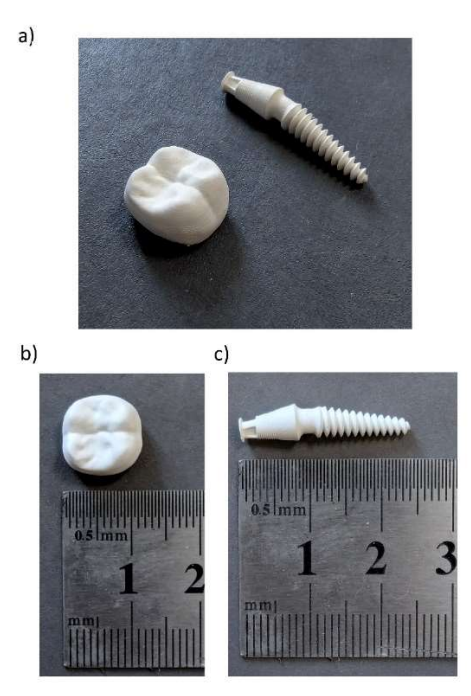


Figure 4. a) Printed zirconia green bodies, b) dental crown and c) dental implant

4. Conclusion

The production of yttrium stabilised zirconia (YSZ) using the vat-photopolymerisation additive manufacturing method holds considerable potential, although it faces substantial challenges due to the inherent properties of yttrium stabilised zirconia powders such as high refractive index (RI) [25]. This study examined the two-dimensional geometric accuracy of ceramic green bodies by analysing the effects of different particle sizes and photoinitiator concentrations under varying exposure times.

The particle size of the ceramic powder plays a critical role in dimensional accuracy as it influences light scattering [47]. Larger particles exacerbate light scattering through diffraction, refraction, and reflection, whereas finer particles reduce diffraction by overlapping scattering volumes. The differences in lateral dimensional error between the two particle sizes become more pronounced at lower photoinitiator concentrations and shorter exposure times. Specifically, the dimensional error nearly doubled when using larger ceramic particles at a photoinitiator concentration of 0.1 wt.% and an exposure time of 20 seconds.

A similar trend was observed in curing depth, although the differences were relatively minor. In addition to particle size, photoinitiator concentration significantly affects both cure depth and geometric error. A higher concentration of photoinitiator generates a greater number of reactive species during UV exposure, initiating polymerisation beyond the intended volume. The lowest dimensional error, while maintaining adequate curing depth, was achieved at the lowest photoinitiator concentration, with values of 0.182 mm and 0.375 mm for small and large particles, respectively.

In contrast, curing depth decreased with increasing photoinitiator concentration, likely due to enhanced light absorption and the resulting inhibition of deeper light penetration within the fast curing time window at the bottom of the suspension. These excess free radicals impede UV light penetration into the ceramic slurry, adversely affecting the system's overall performance. As expected, increasing the exposure time at a fixed light intensity led to greater curing depth and increased horizontal dimensional error, due to the higher total UV energy delivered. Although the dimensional error plateaued with increasing photoinitiator concentration in the case of large particles, variations in exposure energy continued to have an effect.

In conclusion, particle size, photoinitiator content and exposure energy have a significant influence on the cure depth and dimensional accuracy of ceramic green bodies. These factors require further investigation through comprehensive studies. Additionally, further advancements like adding colour pigments aimed at enhancing geometric accuracy should be explored.

Acknowledgment

The authors gratefully acknowledge the Işık Technology (İzmir, Türkiye) for the yttrium stabilised zirconia $(Y_2O_3-ZrO_2)$ support.

Conflict of Interest Statement

The authors declare that there is no conflict of interest

References

- [1] X. Li and Y. Chen, "Vat-Photopolymerization-Based Ceramic Manufacturing," *Journal of Materials Engineering and Performance*, vol. 30, no. 07, pp. 4819–4836, Jul. 2021. doi: 10.1007/s11665-021-05920-z
- [2] Z. Chen et al., "3D printing of ceramics: A review," Journal of European Ceramic Society, vol. 39, no. 4, pp. 661–687, Apr. 2019. doi: 10.1016/j.jeurceramsoc.2018.11.013
- [3] A. Zocca, P. Colombo, C. M. Gomes, and J. G Unster, "Additive Manufacturing of Ceramics: Issues, Potentialities, and Opportunities," *Journal of American Ceramic Society*, vol. 98, no. 7, pp. 1983–2001, 2015. doi: 10.1111/jace.13700
- [4] Y. Lakhdar, C. Tuck, J. Binner, A. Terry, and R. Goodridge, "Additive manufacturing of advanced ceramic materials," *Progress in Materials Science*, vol. 116, p. 100736, Feb. 2021. doi: 10.1016/J.PMATSCI.2020.100736
- [5] K. M. Purlu, S. Dalgac, E. Isik, B. K. Yildiz, and K. Elmabruk, "Preparation and dielectric properties of Al2O3-based ceramic composites with Sm2O3 and ZrO2 additives for terahertz applications," *Ceramic International*, vol. 51, no. 13, pp. 17744–17754, Jan. 2025. doi: 10.1016/J.CERAMINT.2025.01.544
- [6] B. Kafkaslıoğlu Yıldız, H. Yılmaz, and Y. K. Tür, "Evaluation of mechanical properties of Al2O3–Cr2O3 ceramic system prepared in different Cr2O3 ratios for ceramic armour components," *Ceramic International*, vol. 45, no. 16, pp. 20575–20582, Nov. 2019. doi: 10.1016/J.CERAMINT.2019.07.037
- [7] F. Zhang et al., "The recent development of vat photopolymerization: A review," *Additive Manufacturing*, vol. 48, Dec. 2021. doi: 10.1016/j.addma.2021.102423
- [8] M. Pagac et al., "A Review of Vat Photopolymerization Technology: Materials, Applications, Challenges, and Future Trends of 3D Printing," *Polymers*, vol. 13, no. 598, 2021. doi: 10.3390/polym13040598
- [9] O. Santoliquido, P. Colombo, and A. Ortona, "Additive Manufacturing of ceramic components by Digital Light Processing: A comparison between the 'bottom-up' and the 'top-down' approaches," *Journal of European Ceramic Society*, vol. 39, no. 6, pp. 2140–2148, Jun. 2019. doi: 10.1016/J.JEURCERAMSOC.2019.01.044
- [10] K. Zhang, Q. Meng, Z. Qu, and R. He, "A review of defects in vat photopolymerization additive-manufactured ceramics: Characterization, control, and challenges," *Journal of European Ceramic Society*, vol. 44, no. 3, pp. 1361–1384, Mar. 2024. doi: 10.1016/j.jeurceramsoc.2023.10.067
- [11] S. Mamatha, P. Biswas, and R. Johnson, "Digital light processing of ceramics: an overview on process, materials and challenges," Progress in Additive

Manufacturing, vol. 8, no. 5, pp. 1083-1102, Oct. 2023. doi: 10.1007/s40964-022-00379-3

- [12] Z. Wang, W. Yang, Y. Qin, W. Liang, H. Yu, and L. Liu, "Digital micro-mirror device -based light curing technology and its biological applications," *Optics and Laser Technology*, vol. 143, p. 107344, Nov. 2021. doi: 10.1016/J.OPTLASTEC.2021.107344
- [13] A. Al Rashid, W. Ahmed, M. Y. Khalid, and M. Koç, "Vat photopolymerization of polymers and polymer composites: Processes and applications," *Additive Manufacturing*, vol. 47, Nov. 2021. doi: 10.1016/j.addma.2021.102279
- [14] D. C. Watts, "Reaction kinetics and mechanics in photo-polymerised networks," *Dental Materials*, vol. 21, no. 1, pp. 27–35, Jan. 2005. doi: 10.1016/j.dental.2004.10.003
- [15] O. Basar, V. P. Veliyath, F. Tarak, and E. Sabet, "A Systematic Study on Impact of Binder Formulation on Green Body Strength of Vat-Photopolymerisation 3D Printed Silica Ceramics Used in Investment Casting," *Polymers*, vol. 15, no. 14, Jul. 2023. doi: 10.3390/polym15143141
- [16] J. W. Halloran, "Ceramic Stereolithography: Additive Manufacturing for Ceramics by Photopolymerization," *Annual Review of Materials Research*, vol. 46, pp. 19–40, Jul. 2016. doi: 10.1146/annurev-matsci-070115-031841
- [17] P. Sokola et al., "Kinetic stability and rheological properties of photosensitive zirconia suspensions for DLP printing," *Ceramic International*, vol. 49, no. 11, pp. 18502–18509, Jun. 2023. doi: 10.1016/j.ceramint.2023.02.223
- [18] B. Ozkan, F. Sameni, S. Karmel, D. S. Engstrøm, and E. Sabet, "Binder stabilization and rheology optimization for vat-photopolymerization 3D printing of silica-based ceramic mixtures," *Journal of European Ceramic Society*, vol. 43, no. 4, pp. 1649–1662, Apr. 2023. doi: 10.1016/j.jeurceramsoc.2022.11.032
- [19] I. L. de Camargo, M. M. Morais, C. A. Fortulan, and M. C. Branciforti, "A review on the rheological behavior and formulations of ceramic suspensions for vat photopolymerization," *Ceramic International*, vol. 47, no. 9, pp. 11906–11921, May 2021. doi: 10.1016/j.ceramint.2021.01.031
- [20] L. Okoruwa, F. Tarak, F. Sameni, and E. Sabet, "Bridging Experimentation and Computation: OMSP for Advanced Acrylate Characterization and Digital Photoresin Design in Vat Photopolymerization," *Polymers*, vol. 17, no. 2, Jan. 2025. doi: 10.3390/polym17020203
- [21] B. Ozkan et al., "3D printing ceramic cores for investment casting of turbine blades, using LCD screen printers: The mixture design and characterisation," *Journal of European Ceramic Society*, vol. 42, no. 2, pp. 658–671, Feb. 2022. doi: 10.1016/j.jeurceramsoc.2021.10.043
- [22] T. Li et al., "A comprehensive evaluation of vat-photopolymerization resins and alumina slurries for ceramic stereolithography," *Ceramic International*, vol. 49, no. 4, pp. 6440–6450, Feb. 2023. doi: 10.1016/j.ceramint.2022.10.242
- [23] H. Gong et al., "Investigating the correlation and composition of organic components in ZrO2-based slurry on printability improvement and defect suppression of Vat photopolymerization," *Materials Today Communications*, vol. 34, 105149, Mar. 2023. doi: 10.1016/j.mtcomm.2022.105149
- [24] F. Tarak, L. Okoruwa, B. Ozkan, F. Sameni, G. Schaefer, and E. Sabet, "AI for AM: machine learning approach to design the base binder formulation for vat-photopolymerisation 3D printing of zirconia ceramics," *Virtual and Physical Prototyping*, vol. 20, no. 1, Dec. 2025. doi: 10.1080/17452759.2025.2469822
- [25] D. L. Wood and K. Nassau, "Refractive index of cubic zirconia stabilized with yttria," Applied Optics, vol. 21, no. 16, p. 2978, Aug. 1982. doi: 10.1364/AO.21.002978
- [26] X. Wu, C. Xu, and Z. Zhang, "Development and analysis of a high refractive index liquid phase Si3N4 slurry for mask stereolithography," *Ceramic International*, vol. 48, no. 1, pp. 120–129, Jan. 2022. doi: 10.1016/J.CERAMINT.2021.09.087
- [27] M. P. Diebold, "Optimizing the benefits of TiO2 in paints," *Journal of Coatings Technology and Research*, vol. 17, no. 1, Jan. 2020. doi: 10.1007/s11998-019-00295-2
- [28] H. Xing et al., "Effect of particle size distribution on the preparation of ZTA ceramic paste applying for stereolithography 3D printing," *Powder Technology*, vol. 359, pp. 314–322, Jan. 2020. doi: 10.1016/J.POWTEC.2019.09.066
- [29] A. J. Guerra et al., "Optimization of photocrosslinkable resin components and 3D printing process parameters," *Acta Biomater*, vol. 97, pp. 154–161, Oct. 2019. doi: 10.1016/j.actbio.2019.07.045
- [30] P. K. Reddy, P. Gandhi, and G. Singh, "Additive manufacturing of yttria-stabilized zirconia using digital light processing: Green density and surface roughness analysis," *Ceramic International*, vol. 50, no. 13, pp. 22974–22988, Jul. 2024. doi: 10.1016/J.CERAMINT.2024.04.021
- [31] E. Aznarte Garcia, A. J. Qureshi, and C. Ayranci, "A study on material-process interaction and optimization for VAT-photopolymerization processes," *Rapid Prototyping Journal*, vol. 24, no. 9, pp. 1479–1485, Nov. 2018. doi: 10.1108/RPJ-10-2017-0195

- [32] N. D. Borra and V. S. N. Neigapula, "Parametric optimization for dimensional correctness of 3D printed part using masked stereolithography: Taguchi method," *Rapid Prototyping Journal*, Jul. 2022. doi: 10.1108/RPJ-03-2022-0080
- [33] A. Thalhamer, P. Fuchs, L. Strohmeier, S. Hasil, and A. Wolfberger, "A Simulation-Based Assessment of Print Accuracy for Microelectronic Parts Manufactured with DLP 3D Printing Process," 2022 23rd International Conference on Thermal, Mechanical and Multi-Physics Simulation and Experiments in Microelectronics and Microsystems, EuroSimE 2022, Institute of Electrical and Electronics Engineers Inc., 2022. doi: 10.1109/EuroSimE54907.2022.9758869
- [34] C. L. Cramer, J. K. Wilt, Q. A. Campbell, L. Han, T. Saito, and A. T. Nelson, "Accuracy of stereolithography printed alumina with digital light processing," *Open Ceramics*, vol. 8, Dec. 2021. doi: 10.1016/j.oceram.2021.100194
- [35] Y. Y. Cheng, W. F. Lee, J. C. Wang, T. M. G. Chu, J. W. Lai, and P. W. Peng, "Characterization and optical properties of zirconia specimens and ultra-thin veneers fabricated by solvent-based slurry stereolithography with solvent and thermal debinding process," *Ceramic International*, vol. 50, no. 11, pp. 20358–20366, Jun. 2024. doi: 10.1016/J.CERAMINT.2024.03.159
- [36] D. Xiang, Y. Xu, W. Bai, and H. Lin, "Dental zirconia fabricated by stereolithography: Accuracy, translucency and mechanical properties in different build orientations," *Ceramic International*, vol. 47, no. 20, pp. 28837–28847, Oct. 2021. doi: 10.1016/j.ceramint.2021.07.044
- [37] M. Borlaf, A. Serra-Capdevila, C. Colominas, and T. Graule, "Development of UV-curable ZrO2 slurries for additive manufacturing (LCM-DLP) technology," *Journal of European Ceramic Society*, vol. 39, no. 13, pp. 3797–3803, Oct. 2019. doi: 10.1016/J.JEURCERAMSOC.2019.05.023
- [38] L. Zhang, Y. Zeng, H. Yao, Z. Shi, and J. Chen, "Fabrication and characterization of ZrO2(3Y)/Al2O3 micro-ceramic gears with high performance by vat photopolymerization 3D printing," *Ceramic International*, vol. 50, no. 3, pp. 5187–5197, Feb. 2024. doi: 10.1016/J.CERAMINT.2023.11.264
- [39] M. Liu, Y. Wang, H. Zhang, Q. Wei, Z. Liu, and X. Liu, "Influence of particle size distribution on hydroxyapatite slurry and scaffold properties fabricated using digital light processing," *Journal of Manufacturing Process*, vol. 131, pp. 401–411, Dec. 2024. doi: 10.1016/j.jmapro.2024.09.036
- [40] C. Qian, K. Hu, J. Li, P. Li, and Z. Lu, "The effect of light scattering in stereolithography ceramic manufacturing," *Journal of European Ceramic Society*, vol. 41, no. 14, pp. 7141–7154, Nov. 2021. doi: 10.1016/J.JEURCERAMSOC.2021.07.017
- [41] S. Westbeek, J. A. W. van Dommelen, J. J. C. Remmers, and M. G. D. Geers, "Influence of particle shape in the additive manufacturing process for ceramics," *Computers and Mathematics with Applications*, vol. 78, no. 7, pp. 2360–2376, Oct. 2019. doi: 10.1016/j.camwa.2018.08.033
- [42] D. L. Wood, K. Nassau, and T. Y. Kometani, "Refractive index of Y_2O_3 stabilized cubic zirconia: variation with composition and wavelength," *Applied Optics*, vol. 29, no. 16, p. 2485, Jun. 1990. doi: 10.1364/AO.29.002485
- [43] T. Chartier, C. Chaput, F. Doreau, and M. Loiseau, "Stereolithography of structural complex ceramic parts," *Journal of Material Science*, vol. 37, pp. 3141–3147, 2002. doi: 10.1023/A:1016102210277
- [44] S. M. Müller, S. Schlögl, T. Wiesner, M. Haas, and T. Griesser, "Recent Advances in Type I Photoinitiators for Visible Light Induced Photopolymerization," *ChemPhotoChem*, vol. 6, no. 11, Nov. 2022. doi: 10.1002/cptc.202200091
- [45] Serge Gavrilov, "Dental Crown." Accessed: Apr. 28, 2025. [Online]. Available: https://grabcad.com/library/crown-33
- [46] Gopal Mandal, "Dental Implant", Accessed: Apr. 28, 2025. [Online]. Available: https://grabcad.com/library/dental-implant-27
- [47] K. J. Siebert, "Relationship of particle size to light scattering," *Journal of the American Society of Brewing Chemists*, vol. 58, no. 3, pp. 97–100, 2000. doi: 10.1094/asbcj-58-0097

This is an open access article under the CC-BY license

